Adsorption of Te on Ge(001): Density-functional calculations

M. Çakmak,[1] G. P. Srivastava,[2] and Ş. Ellialtıoğlu[3]
[1]*Department of Physics, Art & Science Faculty, Gazi University, Ankara 06500, Turkey*
[2]*School of Physics, University of Exeter, Stocker Road, Exeter EX4 4QL, United Kingdom*
[3]*Department of Physics, Middle East Technical University, Ankara 06531, Turkey*
(Received 26 May 2002; revised manuscript received 21 November 2002; published 20 May 2003)

We present *ab initio* density-functional calculations for the adsorption of Te on the Ge(001) surface. Various possible adsorption geometries for the 0.5-, 0.8-, 1-, and 2-ML (monolayer) coverages of Te have been investigated. Our results for sub-monolayer coverages confirm earlier results as well as provide some new insight into the adsorption of Te. Furthermore, our results for the 2-ML coverage of Te suggest that the bonding between the overlayer and the substrate has changed significantly. This may provide useful information on possible desorption of Te in the form of strongly bonded Te_2 units.

DOI: 10.1103/PhysRevB.67.205314 PACS number(s): 68.35.−p, 73.20.At

I. INTRODUCTION

Physical properties of semiconductor surfaces play an important role in the miniaturization of devices. Adsorption of adatoms can change reconstruction of semiconductor surfaces in many ways by the formation of new bonds. During the last decade many experimental and theoretical studies have been carried out for the atomic and electronic structure of ordered overlayers of elements from different groups of the periodic table on group-IV(001) surfaces. These include the adsorption of group-VI adatoms on the Si(001) and Ge(001) surfaces, such as of S[1–8] and of Se.[9–11] Adsorption of tellurium has attracted much interest recently. Over a wide range of its coverages, Te is known to act as an effective surfactant agent[12] for layer-by-layer growth of Ge on the Si(001) surface, suppressing the growth in island form in the Stranski-Krastanov mode.[13] To understand the role of Te in the Ge/Si heteroepitaxial growth, it is therefore important to examine stable adsorption sites of various coverages of Te on the Si(001) and Ge(001) surfaces.

Using surface extended x-ray-absorption fine-structure (SEXAFS) and x-ray standing waves (XSW) spectroscopies, Burgess *et al.*[14] determined the Te-Si bond length for the Si(001):Te(1×1) surface and as a result concluded that the Te atom were adsorbed in a bridge site. Using the low-energy electron-diffraction (LEED) pattern and scanning tunnel microscope (STM) results, Yoshikawa *et al.*[15] have proposed a missing-row model. Very recently x-ray crystal truncation rod (CTR) measurements by Sakata *et al.*,[16] considered four possible high-symmetry adsorption sites (i.e., the bridge, top, antibridge, and hollow) for Te on the Ge(001) surface. The bridge site adsorption geometry need to be further modified to ensure the reconstruction due to strain on the adlayer. Of the two modified versions of the bridge site models (missing-row and zigzag models), the missing-row model was found to agree best with the CTR data. Ohtani *et al.*[17] and Tamiya *et al.*[18] studied the behavior of Te covered Si(001) surface as a function of increasing temperature by using the LEED, Auger electron spectroscopy (AES), and thermal desorption spectroscopy. These groups started with the room temperature deposition of more than 3 monolayers (ML) of the Te overlayer on a single-domain Si(001)-(1×2) surface. The LEED pattern was observed to change to (1×1) for 1-ML coverage, (2×1) for ~1 ML, (1×3) for 2/3 ML, and (1×2) for 0 ML after annealing at 350 °C, 600 °C, 680 °C, and 800 °C, respectively. The observed streaky LEED patterns were attributed to the continuous shifts of fractional-order spots during the phase transitions from (1×1) to (2×1) and from (1×3) to (1×2). The final (1×2) clean surface was attributed to the formation of a double-domain structure. Lyman *et al.*[19] studied the multiple bonding configurations of Te adsorbed on the Ge(001) surface by using high-resolution XSW and LEED. They observed that close to 1-ML coverage the adsorption takes place at the bridge site, and the 0.5-ML coverage gives rise to a $c(2\times2)$ structure with Ge-Te heterodimers.

On the theoretical side, several first-principles calculations have recently been made to investigate atomic geometry, electronic structure, and energetics of Te adsorption on Si(001) surfaces.[20–22] For the 0.5-ML coverage the adsorption energy of the Te adatom is calculated to be in excess of 2 eV (2.8 eV in Ref. 21 and 4.5 eV in Ref. 22). Takeuchi[20] performed first-principles total-energy calculations for various atomic structure models with different Te coverages (0.25 ML favoring bridge site, 0.8 ML leading to a (5×2) missing-row model, and 1 ML with the adsorption of Te on near bridge sites) on the Si(001) surface, and concluded that the missing-row model plays an important role in the stability of the 1 ML coverage. Takeuchi[23] has also studied the atomic structure of Te on the Ge(001) surface for two different coverages: (i) The 1-ML coverage with Te atoms adsorbed on near bridge sites, giving rise to a slightly distorted surface and (ii) for an annealed system containing the 0.5-ML coverage with Te making a heterodimer with a surface Ge atom resulting into a $c(2\times2)$ structure.

In order to understand the complex adsorption behavior of Te adsorption on Ge(001), in this work, we report further *ab initio* theoretical investigations of the geometrical structure, electronic band structure, and chemical bonding of Te on the Ge(001) surface by considering several plausible adsorption models for 0.5-, 0.8-, 1-, and 2-ML coverages. Our work provides results additional to that presented in the theoretical investigation by Takeuchi.[20] In particular, we have presented the role of Ge-Te heterodimers for submonolayer coverages.

We find that although the bridge model is most favorable structurally and energetically for the 1-ML coverage, unfortunately the resulting band gap is nearly zero at the zone center. For the 2-ML coverage of Te, we find that the bonding between the overlayer and the substrate has changed significantly. This may provide useful information on possible desorption of Te in the form of strongly bonded Te_2 units.

II. METHOD

Our calculations are made using the density-functional theory of Hohenberg, Kohn, and Sham. The electron-ion interaction was considered in the form of *ab initio* norm-conserving pseudopotentials listed by Bachelet, Hamann, and Schlüter.[24] The electron-electron interaction was considered within the local-density approximation (LDA) of the density-functional theory, using the correlation scheme of Ceperley and Alder[25] as parametrized by Perdew and Zunger.[26] Self-consistent solutions to the Kohn-Sham equations were obtained by employing a set of four (four, three, one) special **k** points for 1×1 (2×1, 2×2, 5×1) in the irreducible segment of the surface Brillouin zone.[27] We considered an artificially constructed periodic geometry along the surface normal. The unit cell included an atomic slab with eight layers of the Ge substrate plus a vacuum region equivalent to about six substrate layers in thickness. The two back substrate layers were frozen into their bulk positions, and each Ge atom at the back surface was saturated with two pseudohydrogen (H_{ps}) atoms. All the remaining substrate atoms, the adsorbate atoms, and the saturating H_{ps} atoms were allowed to relax into their minimum-energy positions using a conjugate gradient method.[28]

Single-particle wave functions were expanded using a plane-wave basis up to a kinetic energy cutoff of 8 Ry. This cutoff was found to be adequate for the structural studies as well as the electronic structure. We do not find any significant changes in the structural parameters when the energy cutoff is increased from 8 Ry to 12 Ry. Our earlier works[29,30] have also concluded that the structural results are well converged for H_2S or S chemisorbedsemiconductor surfaces with 8 Ry energy cutoff. Similar observations regarding the convergence of results for the hydrogen overlayer systems using 8–10 Ry cutoff have been made by other groups,[31,32] as well. With 8 Ry cutoff, the theoretical lattice constant for bulk Ge is 5.53 Å. The convergence of results with 8 Ry cutoff was tested for one of the structural models considered in this work, viz. the 2-ML coverage of Te on the Ge(001) surface (see Sec. III D). While the total energy has not sufficiently converged at 8 Ry, the essential results have. For example, the calculated band gap is 0.28, 0.19, and 0.15 eV for 6, 8, and 10 Ry energy cutoffs, respectively. Similarly, the vertical separation between the lower-lying Te and the top-layer Ge is 1.52, 1.54, and 1.54 Å, and the vertical distance between the two Te atoms is 2.23, 2.23, and 2.27 Å for 6, 8 and 10 Ry cutoffs, respectively.

Although calculations of quasiparticle surface band structure have not been attempted in this work, the solutions of the Kohn-Sham equations withing the local-density approximation have been used to discuss orbital nature, chemical bonding, and *trends* in surface electronic band structure. These attempts are justified by noting that quasiparticle band-structure results may quite well be considered as ''scissored'' versions of LDA results, and also that the the LDA wave funtions represent the quasiparticle wave functions very well.[28] In any case, in discussing the results presented in this section, it will be helpful to note that the LDA band gap obtained for bulk Ge at 8 Ry energy cutoff at the theoretical lattice constant of 5.53 Å is nearly 0.6 eV.

III. RESULTS AND DISCUSSIONS

In this section, we present and discuss results for various plausible adsorption sites on Ge(001) for Te with coverages 0.5, 0.8, 1, and 2 ML. Preferred structures for the temperature-dependent and coverage-dependent adsorption of Te on Ge(001) can be listed as follows: (i) bridge site as revealed by XSW, SEXAFS, and STM measurements,[14] (ii) missing row model (MRM) with (5×1) surface reconstruction as concluded by XSW, LEED,[19] and CRT,[16] (iii) MRM with (5×2) geometry as suggested by the STM and the LEED measurements,[15] and backed by theory,[20] and (iv) $c(2\times2)$ geometry as observed by AES[17] and confirmed by *ab initio* calculations.[23] In this work, we have attempted to study seven different configurations including (i), (ii), and (iv) mentioned above. These are classified in the order of increasing coverage of Te and are described in the following sections.

A. High-temperature-annealed phase with 0.5 ML Te on Ge(001)

The LEED investigations of high-temperature-annealed samples indicate both[33] (2×2) and streaky[19] $c(2\times2)$ structural patterns for 0.5-ML coverage of Te on Ge(001). Consistent with these patterns, we have considered several atomic configurations with (2×2) and $c(2\times2)$ periodicities in what follows. On the theoretical side Takeuchi[20] has earlier considered three different configurations with a $c(2\times2)$ periodicity: (a) Te atoms adsorbed on the top of unbroken Ge-Ge dimers, (b) Te atoms located in cave sites, with the Ge-Ge dimers intact, and (c) a structure formed by the mixed Ge-Te dimers. He found the last structure to be the most stable one.

1. Mixed Ge-Te *dimer geometry within* $c(2\times2)$ *and* (2×2)

In this work, we have considered a total of five models for the 0.5-ML Te on the Ge(001) surface, leading to the $c(2\times2)$ and (2×2) surface reconstructions. The first three, shown in Fig. 1 (labeled models I–III), contain mixed Ge-Te dimers. Model I is characerized by a parallel arrangement of the Ge-Te dimers, in model II the Ge and Te components of neighboring dimers are swapped, and in model III the neighboring dimers are positioned in a staggered manner. The other two models will be discussed in the following section.

We have performed energy minimizations starting from these geometries with different starting phases of the Ge-Te dimers. We find that the mixed Ge-Te dimer on the $c(2\times2)$ surface reconstruction (model III) is energetically fa-

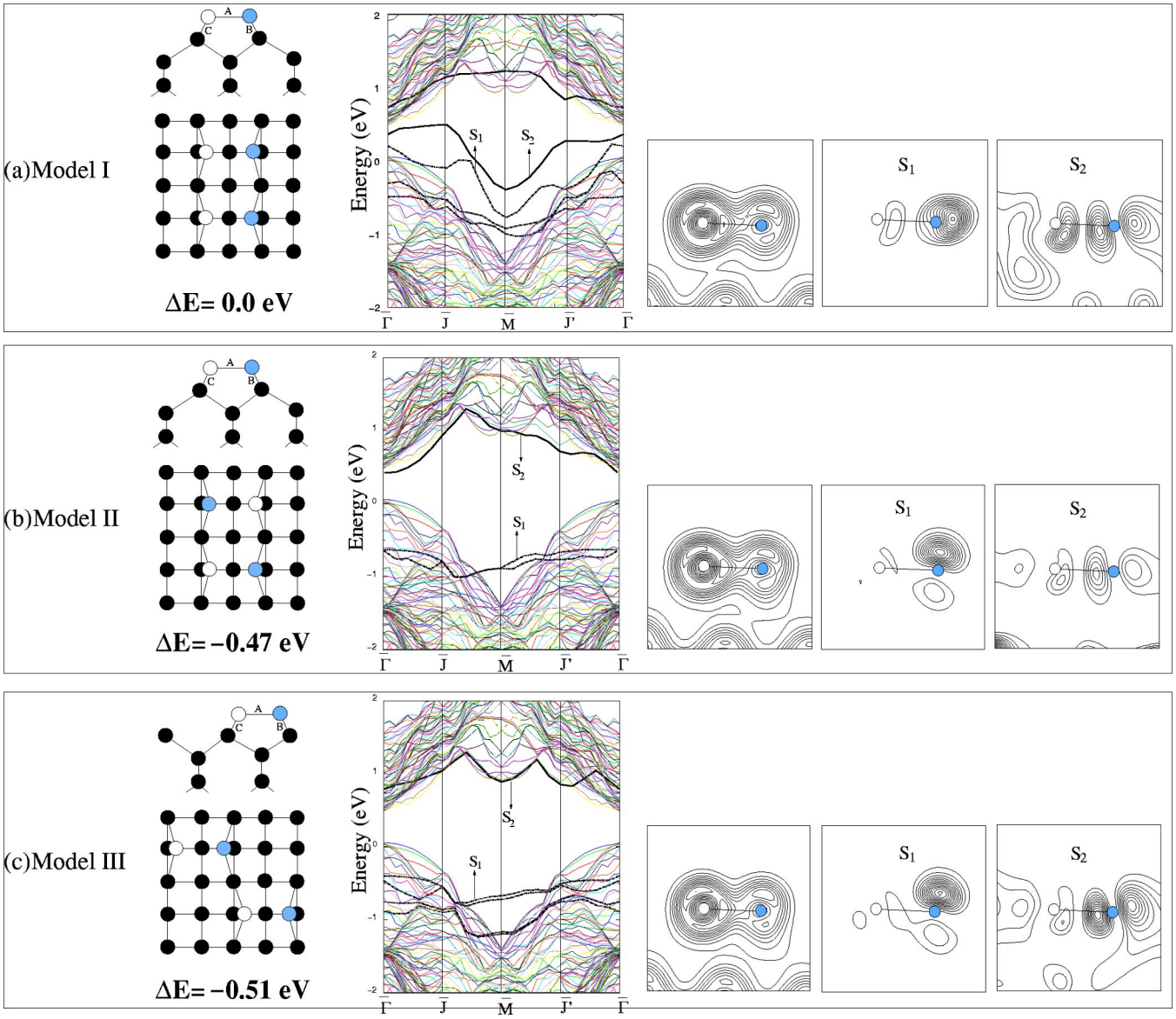

FIG. 1. (a) Schematic top and side views of the 0.5-ML Te coverage of the mixed Ge-Te/Ge(001)-(2×2) with a parallel arrangement of Ge-Te dimers (model I), its related band structure, electronic total charge-density and electronic charge-density plots of the individual states, (b) same results for model II : 0.5-ML Te coverage of the mixed Ge-Te/Ge(001)-(2×2) characterized by neighboring dimers with the Ge and Te components swapped, and (c) that of model III: 0.5-ML Te coverage of the mixed Ge-Te/Ge(001)-c(2×2) with neighboring dimers positioned in a staggered manner. The thick dashed lines represent occupied surface bands and the thick solid lines represent unoccupied surface states. The thin lines represent the two-dimensional projection of the band structure for bulk Ge. The filled and open circles represent the Ge atoms. The gray circles represent the Te atoms.

vorable by 0.51 eV/dimer, compared to the mixed Ge-Te dimer on the (2×2) surface reconstruction (model I). Upon relaxation, in all three cases, we find that the Ge-up configuration is more stable than the Te-up configuration. For the c(2×2) surface reconstruction, we have found this asymmetry to be slightly less than 5° in the tilt angle, with the Ge atom lying 0.19 Å higher in the surface normal direction than the Te atom. This vertical buckling has been calculated by Takeuchi[20] as 0.21 Å. The other key structural parameters are presented in Table I, where we have compared our results with those of Takeuchi's first-principles total-energy calculations, which are similar to ours. For model III, the calculated Ge-Te dimer bond length of 2.77 Å, somewhat bigger than the sum of their corresponding covalent radii (viz. 2.54 Å,[34]) is in good agreement with Takeuchi's value of 2.84 Å. Model II is found to be almost as energetically stable as model III. This suggests that the Ge-Te heterodimer formation prefers either an alternately positioned (II) or a staggered arrangement (III).

Information regarding the band structure of Te covered Ge(001) surfaces is missing from the literature. We have presented the electronic band structure for the three models of Ge-Te mixed dimer on the (2×2) and c(2×2) surfaces in Fig. 1. From their corresponding band structures, one can see that the fundamental band-gap region is free of the surface states for models II and III, while one observes an overlap

TABLE I. Key structural parameters and relative energy for the mixed Ge-Te dimer on the Ge(001)-(2×2) and Ge(001)-$c(2\times2)$ surfaces. The labels *A*, *B*, and *C* are shown in Fig. 1. The vertical buckling of the dimer (with Ge in up position) is $d_{12,\perp}$.

System	*A* (Å)	*B* (Å)	*C* (Å)	$d_{12,\perp}$ (Å)	Relative *E* (eV)
Model I	2.75	2.61	2.46	0.19	0.00
Model II	2.74	2.65	2.45	0.17	−0.47
Model III	2.77	2.66	2.47	0.19	−0.51
Ref. 23: Theory	2.84	2.71	2.52	0.21	

between the highest occupied state and the lowest unoccupied surface state for model I. Therefore, we can explicitly say that models II and III are semiconducting in nature, while model I is not. We have also depicted the related orbital nature of the surface states for the highest occupied and the lowest unoccupied states for models I, II, and III together with their total charge-density plots in Figs. 1(a–c). All these models have similar total charge-density distribution, and show similar orbital nature for the highest occupied S_1 and the lowest unoccupied S_2 states. The highest occupied S_1 state for all the three models results from the occupied sp_z orbital at the Te dimer component, and the lowest unoccupied state S_2 is contributed by the p_x-p_y orbitals of the Te atom.

2. Antibridge and bridge geometries for the 0.5 ML Te *coverage*

As we have mentioned in the preceding section, we have considered two other geometries with a (2×2) periodicity. These involve adsorption of the Te atoms with the Ge-Ge dimer intact, shown in Fig. 2, based on an antibridge geometry (two Te atoms saturate the four dangling bonds at two neighboring Ge-Ge dimers in a row (model IV) and a bridge geometry (Te atoms are on the top between the Ge-Ge dimers (model V) in which all the Ge atoms are fourfold coordinated and the Te atoms are two-fold coordinated, thus leaving no unsaturated dangling bonds in the system. The bridge model has also been considered in the theoretical works mentioned earlier for the Si(001)/Te system.[20,21] The antibridge model, however, is found to be energetically more favorable, having a total energy that is 0.44 eV lower than the bridge model. Upon Te adsorption, the Ge-Ge dimer becomes symmetric and is slightly elongated to a length of 2.45 Å for the antibridge model, and to 2.36 Å for the bridge model. The average perpendicular distance between the Ge-Ge dimer and the Te atom ($d_{12,\perp}$) is much larger for model V than for model IV. The relative increase in the total energy for model V compared to model IV is largely due to the compressed dimer for the former (Table II).

The electronic band structure for the anti-bridge model is presented in Fig. 3. We have identified a total of three occupied and one unoccupied surface states around the fundamental band gap region. Our calculations have produced a band gap at the zone center ($\bar{\Gamma}$) of ≈0.19 eV, much smaller than the bulk band gap within the same calculational details, indicating that the adsorption of Te leaves the surface electronically nonpassivated. Figure 3 also presents charge-density plots for this system. The highest occupied surface state S_1 is contributed by both the $ss\sigma$ bonding within the Ge-Ge dimer and the $pp\sigma$ bonding between the two Te atoms within a surface unit cell. The second occupied state, labeled S_2, originates from the p_z orbitals of each of the Te atoms. In addition to the occupied states, we have also depicted the lowest unoccupied surface state (labeled S_3), which has a large Te sp_z contribution. Since the Ge-Ge $ss\sigma$ band on the Ge(001)-(2×1) surface lies well below the bulk valence-band maximum, we suggest that the nonpassivating behavior of this model results from the Te-Te $pp\sigma$ bonding and sp_z nonbonding orbitals. It is interesting to compare the total energies and band structures for models III and IV. We find that model III is energetically more favorable by 0.86 eV/(2×2) cell. This is due to the Te-Ge heterodimer formation, which fulfills the electron counting rule and results in fully occupied dangling bonds at both components of the dimer.

3. Energetic comparison of different geometries for the 0.5 ML Te *coverages*

In order to establish the most likely candidate for the stable geometry for 0.5-ML coverage of Te on Ge(001), we express the adsorption energy per Te atom as

$$E_b = E_T[\mathrm{Ge}] + E_a[\mathrm{Te}] - E_T[\mathrm{Ge+Te}], \tag{1}$$

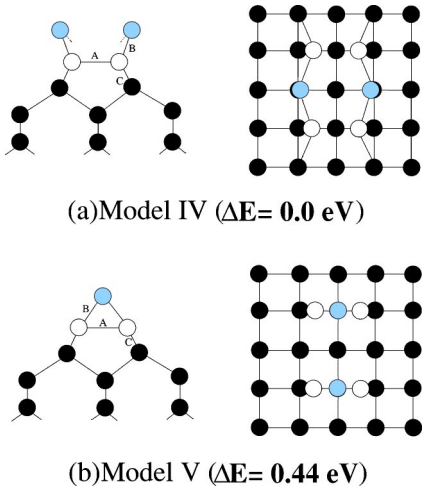

FIG. 2. Schematic side and top views of the 0.5-ML Te coverage of (a) the antibridge model for the Ge(001)-(2×2) surface (model IV), and (b) the 0.5-ML Te at the bridge position on the Ge-Ge dimer within Ge(001)-(2×2) surface (model V).

TABLE II. Key structural parameters and relative energies for models IV and V. The labels *A*, *B*, and *C* are shown in Fig. 2. $d_{12,\perp}$ is the average perpendicular distance between the Ge-Ge dimer and the Te atom.

System	*A* (Å)	*B* (Å)	*C* (Å)	$d_{12,\perp}$ (Å)	Relative *E* (eV)
Antibridge (model IV)	2.45	2.61	2.38	1.86	0.00
Bridge (model V)	2.38	2.55	2.36	2.26	0.44

where E_T[Ge] is the total energy of the Ge slab, E_T[Ge +Te] is the total energy of the Te adsorbed Ge slab, and E_a[Te] is the energy of a single isolated Te atom. The total energies E_T[Ge] and E_T[Ge+Te] were calculated in the same size supercell. The atomic energy E_a[Te] was calculated by placing the diatomic Te_2 molecule inside a repeated cubic box of size 15 Å. The structure was relaxed towards its minimum-energy configuration. For Te_2 the relaxed bond length is 2.54 Å, which is somewhat smaller than twice its tetrahedral radius (2.64 Å) but is in excellent agreement with twice of its normal double bond radius (2.54 Å)[34] and also in good agreement with the calculated value of 2.56 Å by Sen *et al.*[22] The atomic energy E_T[Te] was taken as half of the total energy of the Te_2 molecule thus calculated.

We have calculated the adsorption energy values (in eV per Te atom) of 3.41, 3.63, and 4.06 for models V, IV, and III, respectively. These values are in the same range as calculated in Refs. 21 and 22 for Te adsorption on Si(001) within model V (i.e., for the adsorption of Te on Si-Si dimers). Since our results show a clear increase in the binding energy of Te for model III over model V, we conclude that for the submonolayer coverages formation of Te-Ge heterodimers is more stable than geometries based on the adsorption of the Te atoms on Ge-Ge dimers. This conclusion seems contarry to the adsorption of Te on Si(001), for which formation of Te-Si heterodimers was found to be energetically unfavorable.[21]

B. Low-temperature-annealed phase with the 0.8-ML Te on Ge(001)

As mentioned in Sec. I, in saturation limit the low-temperature annealing phase corresponds to 0.8-ML coverage of Te. This can be accommodated within a Te missing-row model. Depending on the position and orientation of the Ge-Ge dimer in the missing Te row, two different surface reconstructions have been proposed. Takeuchi[20] has proposed a model in which Te rows are oriented 90° to the Ge-Ge dimer rows, i.e., the Ge-Ge dimer is in the *antibridge* direction making the surface unit cell to be (5×2) reconstructed. The surface unit cell contains eight Te atoms, and eight Ge atoms, and a Ge-Ge dimer in the top substrate layer. A more convincing Te missing-row model has been proposed by Sakata *et al.*,[16] in which the Ge-Ge dimers lie in the Te *inter-row* direction, leading to a (5×1) surface reconstruc-

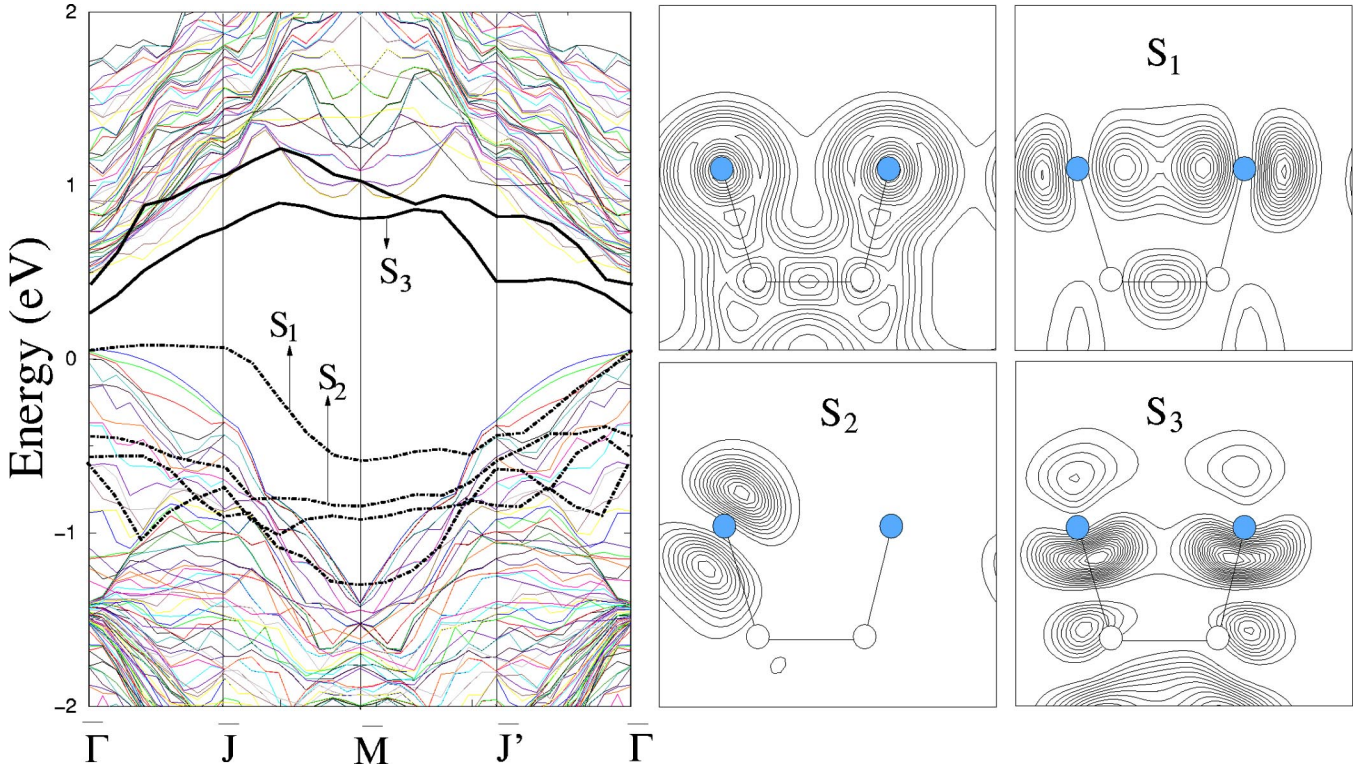

FIG. 3. Calculated band structure for model IV shown in Fig. 2(a). The electronic total charge-density and electronic charge-density plots of the individual states of model IV at $\bar{M}$ are presented on the plane cutting obliquely through the Te atoms with the Ge-Ge dimer.

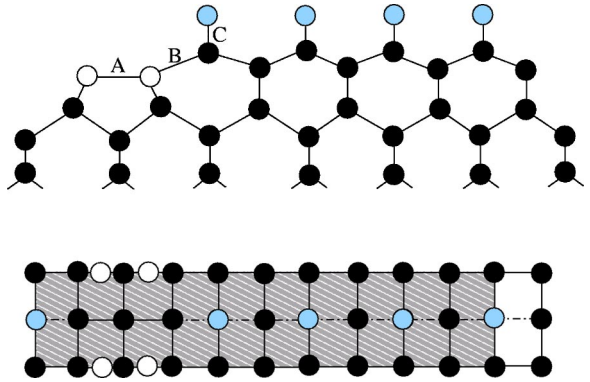

FIG. 4. Schematic side and top views of the missing-row model Te(0.8 ML)/Ge(001)-(5×1).

tion. The surface unit cell contains four Te atoms, four Ge atoms in the top substrate layer, and a Ge-Ge dimer below the top substrate layer in the missing Te row. In the present work, we *only* consider the model proposed by Sakata *et al.*, which is shown in Fig. 4.

Within the model proposed by Sakata *et al.*, we started our theoretical modeling by initially considering the Ge-Ge dimer as *symmetric*. Upon relaxation, we found that the Ge-Ge dimer was pushed inwardly, towards the Ge layer below. The perpendicular distance between the Ge-Ge dimer and the lower Ge layer is shortened from 1.32 Å to 0.90 Å. The Ge-Ge bond length is found to be 2.27 Å, smaller than its clean surface value of 2.38 Å.[28] Again, within the model proposed by Sakata *et al.*, second theoretical modeling was carried out by initially considering the Ge-Ge dimer with *a small tilt angle* of 6° with respect to the surface. Interestingly, upon relaxation, the Ge-Ge dimer was found to be broken and was found to be 0.75 eV/(5×1) cell energetically more favorable than the symmetric Ge-dimer model just considered. This is actually an intermediate step towards the formation of the monolayer bridge model shown in Fig. 5. When there are enough Ge and Te atoms at the surface, we will see that the monolayer bridge model will evolve as discussed in the following section.

C. The Ge(001):Te(1×1) phase

As concluded by Lyman *et al.* the Te coverage saturates at nearly 1 ML, leading to at least a locally observed (1×1) geometry. The monolayer bridge model maintains fourfold coordination of all the Ge atoms and twofold coordination of the Te atoms, with the Te atoms sitting above the topmost Ge atoms in the bridge absorption sites, as shown in Fig. 5. This is the acceptable model for S and Se on Si(001) and Ge(001).[7,11] The structural parameters listed in Table III are as follows: The calculated perpendicular distance between the Ge and Te atoms being 1.64 Å is somewhat larger than the experimentally measured value of 1.52±0.02 Å[20] (and references therein) and the theoretically calculated value of 1.54 Å reported by Takeuchi.[20] The calculated bond length between the Ge and Te atoms is 2.55 Å, very close to Takeuchi's value of 2.59 Å.[20]

The energy bands for this case, presented in Fig. 5, indicate that the band gap at $\bar{\Gamma}$ is nearly zero. We have identified two occupied surface states below the valence-band maximum, labeled S_1 and S_2 and one unoccupied surface state in the gap, labeled as S_3. An inspection of the total charge density shown in Fig. 5, which is plotted on the plane cutting vertically through the Te atom and the first topmost Ge layer, reveals that the Ge-Te bond is polar with some degree of polarity towards the Te atom. This is caused by a large degree of covalency plus some ionic character, giving rise to a shift in the charge-density peak towards the more electronegative Te atom. The highest occupied surface state S_1 is primarily derived from the p_z orbital of the Te atom. The surface state S_2, on the other hand, has a complex antibonding nature. The lowest unoccupied state S_3 is derived from the lone-pair orbitals p_y of the Te atom. The near collapse of the band gap suggests that either the 1-ML coverage of Te, or the bridge model, is unfavorable. Considering the former as-

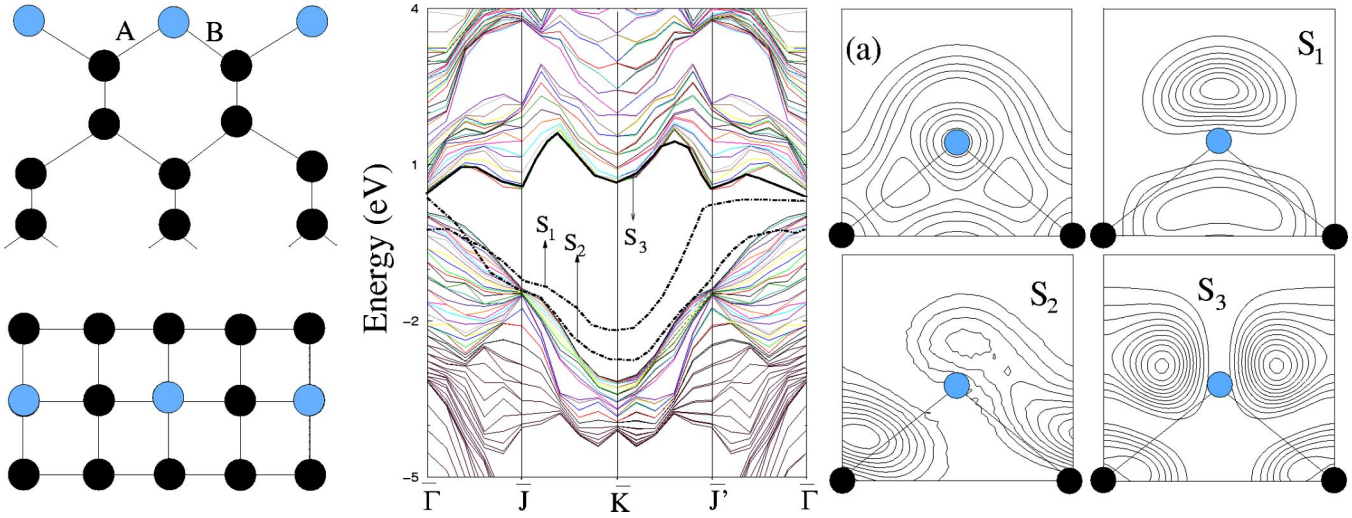

FIG. 5. Schematic side and top view of 1-ML-bridge model-Te(1 ML)/Ge(001)-(1×1) with its band structure and its related electronic total charge density and the individual surface states.

TABLE III. Key structural parameters for the Te/Ge(001)-(5×1) missing dimer model, 1-ML Te-bridge model and the Te embedded into the Ge substrate. The labels *A*, *B*, and *C* are shown in Fig. 4. $d_{12,\perp}$ is the average perpendicular distance between the Ge atom and the Te atom.

System	*A* (Å)	*B* (Å)	*C* (Å)	$d_{12,\perp}$ (Å)
Missing row model-Te(0.8 ML)/Ge(001)-(5×1)	2.66	2.64	2.60	
Bridge model-Te(1 ML)/Ge(001)-(1×1)	2.55	2.55		1.64
Reference 20: Theory	2.59	2.59		1.54
Reference 19: Experiment				1.52±0.02
Embedded model-Te(2 ML)/Ge(001)-(1×1)	2.66	2.66	2.59	

sumption being true, our work can be interpreted to provide support for the experimental observations that the 0.8 ML rather than the 1-ML coverage of Te is more likely to take place on Ge(001).

D. The Ge(001) surface with the 2-ML coverage of Te

The Ge(001) surface with the 2-ML coverage of Te may not be as ideally coordinated as the 1-ML covered surface, as shown in Fig. 6. Our earlier work[7] and experimental works by Papageorgopoulos *et al.*[5,11] for the adsorption of S and Se on Si(001) clearly demonstrate that at room temperature the coverage above 1 ML leads to embedding of the second layer of the S and Se adatoms into the Si bulk near the surface. This led us to study the embedded model for Te on Ge(001). However, upon relaxation the bonding structure between the overlayer and the substrate has been observed to change significantly. The schematics of the relaxed geometry is given in Fig. 6, which shows that the Te atoms in the embedded sites are pushed out towards the surface, leaving two Te atomic layers well separated from the Ge surface layer. This suggests that the second ML of Te grows epitaxially on the top of its first ML. The vertical displacement between the first and second layer Ge atoms is shortened from 1.57 Å to 1.33 Å. The Te-Te, Ge-Te and Ge-Ge bond lengths are found to be 2.59, 2.66, and 2.36 Å, respectively. The value of 2.66 Å for the Ge-Te bond is obviously somewhat bigger than the sum of their covalent radii ($r_{\text{Ge-Te}}=2.54$ Å). We suggest that the desorption of Te double layer may take place at an appropriately high temperature, containing strongly bonded Te_2 units, and the remaining substrate may then result in the bare Ge(001) surface with (2×1) or $c(2\times2)$ reconstruction.[35]

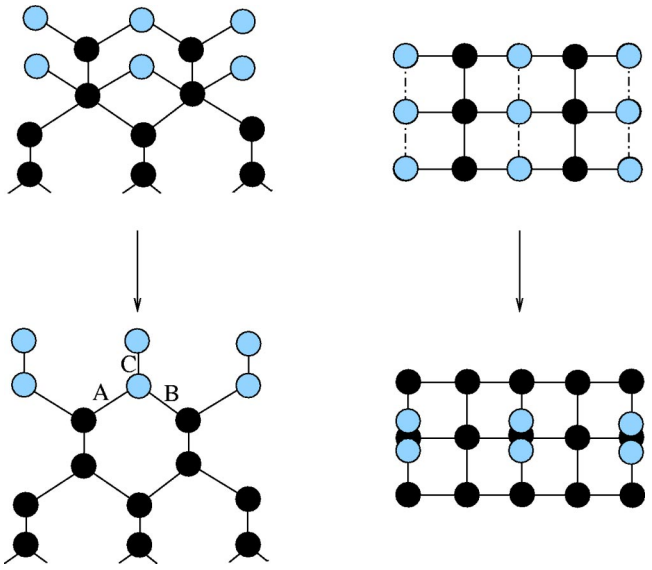

FIG. 6. Schematic side and top view of the embedded model-Te(2 ML)/Ge(001)-(1×1).

E. Relative stability of the 0-ML, 1-ML, and 2-ML Te phases

The stable surface reconstruction is the one with the lowest surface energy. Total energies for different structures can only be compared when the structures share the same stoichiometries. However, nonstoichiometric surfaces can be considered by allowing the surface to exchange atoms with a reservoir, which is characterized by a chemical potential.[35] As the half and full monolayer phases share different stoichiometries, their relative energetic stabilities can be studied by examining the free energy of each system.

In our case, due to the varying numbers of the Te and Ge atoms per unit cell the comparison of the total energy for the different adsorption configurations considered here has to take into account the chemical potentials of the respective species. The surface free energy of a supercell may be written as

$$F = E - \sum_i n_i \mu_i , \tag{2}$$

where n_i is the number of atoms and μ_i is the chemical potential of the *i*th species. The total energy of the supercell *E* is taken from our *ab initio* calculations. Since the Te atoms at the surface must be in equilibrium with the bulk, μ_{Ge} must equal μ_{Ge}^{bulk}, so we have

$$F = E' - n_{\text{Te}}\mu_{\text{Te}} , \tag{3}$$

where $E' = E - n_{\text{Ge}}\mu_{\text{Ge}}^{bulk}$ is a constant for a chosen structure. Thus, the free energy of the system can be considered to vary linearly with the surface chemical potential μ_{Te} of Te.

To be entirely consistent with respect to numerical details, we calculated the bulk Ge chemical potential using the same size supercell and the same number of special **k** points as described in Sec. II. The Te chemical potential should be considered with the constraint $\mu_{\text{Te}} - \mu_{\text{Te}}^{bulk} \leqslant 0$, where μ_{Te}^{bulk} is the bulk Te chemical potential. We have considered a reasonable range for $\mu_{\text{Te}} - \mu_{\text{Te}}^{bulk}$, with μ_{Te}^{bulk} considered for a

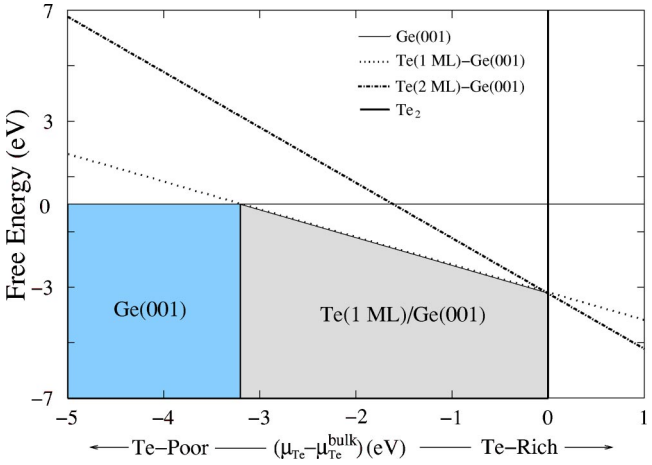

FIG. 7. The surface free energy of different monolayers of Te on Ge(001)-(1×1) plotted against Te chemical potential.

thermodynamically stable form of Te. The energy we calculated is almost certainly higher than the true energy, but the weak van der Waals Te_2-Te_2 interaction in the three-dimensional structure means that such an overestimation should be small. Based upon these results, we have considered the value of μ_{Te} not to exceed μ_{Te_2} (which is shown as the limiting case in Fig. 7.). In other words, our estimate for μ_{Te}^{bulk} is μ_{Te_2}.

We performed calculations for the 1×1 surfaces with 0-, 1-, and 2-ML coverages of Te on Ge(001). In Fig. 7 we have plotted the free energy F as a function of $\mu_{Te}-\mu_{Te}^{bulk}$ in the range 1.0–5.0 eV. It is clear that the 2-ML phase is never the lowest-energy phase at any accessible Te chemical potential. For $\mu_{Te}-\mu_{Te}^{bulk}<-3.18$ eV (i.e., in the Te poor limit) the clean Ge(001) surface is energetically favorable. For $\mu_{Te}-\mu_{Te}^{bulk}>-3.18$ eV the monolayer Te phase is favourable. This seems just as interesting a result to us thermodynamically as to disallow the 2-ML phase. The thermodynamic instability of the 2-ML Te phase is consistent with the above-mentioned experimental poor evidence and the theoretical discussion regarding desorption of Te in the form of stongly bonded Te_2 units. Our energetically more favorable case for 1 ML, i.e., Te (1 ML)/Ge(001)-(1×1), was also found for the Si surface by Miwa and Ferraz.[21]

IV. SUMMARY

We have made a detailed investigation of the Te adsorption, with various geometries corresponding to 0.5 ML, 0.8 ML, 1 ML, and 2 ML of Te on the Ge(001) surface by using *ab initio* density-functional calculations. Our work for submonolayer coverages has confirmed earlier theoretical results as well as has proposed possible geometries with passivating character. With increasing Te coverage, the 0.8 ML rather than the 1-ML coverage of Te is more likley to take place. Our results also suggest that for the 2-ML coverage Te atoms prefer to be adsorbed as a double layer, which may provide support for desorption of Te as strongly bonded Te_2 units at appropriately high temperatures, leaving the Ge(001) surface bare with (2×1) or $c(2\times2)$ reconstruction.

ACKNOWLEDGMENTS

This research was supported by TÜBİTAK Grants No. TBAG-1950 (100T073) and No. TBAG-2036 (101T058). Also, this work at Gazi University was supported by Turkish Republic of Prime Ministry state Planning Organization (Project No 2001K120590).

[1] E. Kaxiras, Phys. Rev. B **43**, 6824 (1991).
[2] P. Krüger and J. Pollman, Phys. Rev. B **47**, 1898 (1993).
[3] P. Moriarty, L. Koenders, and G. Hughes, Phys. Rev. B **47**, 15 950 (1993).
[4] G.W. Anderson, M.C. Hanf, P.R. Norton, Z.H. Lu, and M.J. Graham, Appl. Phys. Lett. **66**, 1123 (1994).
[5] A. Papageorgopoulos, A. Corner, M. Kamaratos, and C.A. Papageorgopoulos, Phys. Rev. B **55**, 4435 (1997).
[6] M. Göthelid, G. LeLay, C. Wigren, M. Björkqvist, M. Rad, and U.O. Karlsson, Appl. Surf. Sci. **115**, 87 (1997).
[7] M. Çakmak and G.P. Srivastava, J. Appl. Phys. **84**, 6070 (1998).
[8] J. Roche, P. Ryan, and G. Hughes, Surf. Sci. **465**, 115 (2000).
[9] R.D. Bringans and M.A. Olmstead, Phys. Rev. B **39**, 12 985 (1989).
[10] Y.-J. Zhao, P.-L. Cao, and G. Lai, J. Phys.: Condens. Matter **10**, 7769 (1998).
[11] A.C. Papageorgopoulos and M. Kamaratos, Surf. Sci. **466**, 173 (2000).
[12] H.J. Osten, J. Klatt, G. Lippert, E. Bugiel, and S. Higuchi, J. Appl. Phys. **74**, 2507 (1993).
[13] S. Higuchi and Y. Nakanishi, Surf. Sci. Lett. **254**, L465 (1991).
[14] S.R. Burgess, B.C.C. Cowie, S.P. Wilks, P.R. Dunstan, C.J. Dunscombe, and R.H. Williams, Appl. Surf. Sci. **104/105**, 152 (1996).
[15] S.A. Yoshikawa, J. Nogami, C.F. Quante, and P. Pianetta, Surf. Sci. **321**, L183 (1994).
[16] O. Sakata, P.F. Lyman, B.P. Tinkham, D.A. Walko, D.L. Marasco, T.-L. Lee, and M.J. Bedzyk, Phys. Rev. B **61**, 16 692 (2000).
[17] T. Ohtani, K. Tamiya, Y. Takeda, T. Urano, and S. Hongo, Appl. Surf. Sci. **130-132**, 112 (1998).
[18] K. Tamiya, T. Ohtani, Y. Takeda, T. Urano, and S. Hongo, Surf. Sci. **408**, 268 (1998).
[19] P.F. Lyman, D.L. Marasco, D.A. Walko, and M.J. Bedzyk, Phys. Rev. B **60**, 8704 (1999).
[20] N. Takeuchi, Phys. Rev. B **60**, 4796 (1999).
[21] R.H. Miwa and A.C. Ferraz, Surf. Sci. **449**, 180 (2000).
[22] P. Sen, S. Ciraci, I.P. Batra, C.H. Grein, and S. Sivananthan, Surf. Sci. **519**, 79 (2002).
[23] N. Takeuchi, Surf. Sci. **426**, L433 (1999).
[24] G.B. Bachelet, D.R. Hamann and M. Schlüter, Phys. Rev. B **26**, 4199 (1982).
[25] D.M. Ceperley and B.I. Alder, Phys. Rev. Lett. **45**, 566 (1980).

[26] J.P. Perdew and A. Zunger, Phys. Rev. B **23**, 5048 (1981).
[27] R.A. Evarestov and V.P. Smirnov, Phys. Status Solidi **119**, 9 (1983).
[28] G. P. Srivastava, *Theoretical Modelling of Semicondcutor Surfaces* (World Scientific, Singapore, 1999).
[29] M. Çakmak and G.P. Srivastava, Phys. Rev. B **60**, 5497 (1999).
[30] M. Çakmak and G.P. Srivastava, Phys. Rev. B **61**, 10 216 (2000).
[31] S. Hong and M.Y. Chou, Phys. Rev. B **58**, R13 363 (1998).
[32] S. Jeong and A. Oshiyama, Phys. Rev. B **58**, 12 958 (1998).
[33] M.R. Bennett, C.J. Dunscombe, A.A. Cafolla, J.W. Cairns, J.E. Macdonald, and R.H. Williams, Surf. Sci. **380**, 178 (1997).
[34] G. Burns, *Solid State Physics* (Academic, New York, 1990).
[35] G.-X. Qian, R.M. Martin, and D.J. Chadi, Phys. Rev. B **38**, 7649 (1988).